Emergent SO(5) Symmetry at the Néel to Valence–Bond–Solid Transition

Adam Nahum,[1] P. Serna,[2] J. T. Chalker,[2] M. Ortuño,[3] and A. M. Somoza[3]

[1]*Department of Physics, Massachusetts Institute of Technology, Cambridge, MA 02139, USA*
[2]*Theoretical Physics, Oxford University, 1 Keble Road, Oxford OX1 3NP, United Kingdom*
[3]*Departamento de Física – CIOyN, Universidad de Murcia, Murcia 30.071, Spain*
(Dated: August 28, 2015)

We show numerically that the 'deconfined' quantum critical point between the Néel antiferromagnet and the columnar valence–bond–solid, for a square lattice of spin-1/2s, has an emergent SO(5) symmetry. This symmetry allows the Néel vector and the valence-bond-solid order parameter to be rotated into each other. It is a remarkable 2+1–dimensional analogue of the SO(4) = [SU(2) × SU(2)]/$\mathbb{Z}_2$ symmetry that appears in the scaling limit for the spin–1/2 Heisenberg chain. The emergent SO(5) is strong evidence that the phase transition in the 2+1D system is truly continuous, despite the violations of finite-size scaling observed previously in this problem. It also implies surprising relations between correlation functions at the transition. The symmetry enhancement is expected to apply generally to the critical two-component Abelian Higgs model (non-compact CP^1 model). The result indicates that in three dimensions there is an SO(5)-symmetric conformal field theory which has no relevant singlet operators, so is radically different to conventional Wilson-Fisher-type conformal field theories.

Many condensed matter systems show higher symmetry in the infrared than they do in the ultraviolet. The liquid-gas critical point is a classical example: although there is no microscopic $\mathbb{Z}_2$ symmetry exchanging liquid-like and gas-like configurations, the fixed point has an emergent $\mathbb{Z}_2$ symmetry and is simply the Ising fixed point. Microscopically this fixed point is perturbed by operators which break the $\mathbb{Z}_2$ symmetry, but it nevertheless governs the critical behaviour because these perturbations are irrelevant under the renormalisation group.

To reach this critical point two variables, say temperature and the pressure, must be tuned. The spin-1/2 Heisenberg chain provides an example of emergent symmetry without such fine-tuning in a quantum setting. The ground state of this model is well known to be critical. Its microscopic symmetries are SU(2) spin rotations, together with spatial symmetries. However the scaling limit of the spin-1/2 chain is the SU(2)$_1$ Wess-Zumino-Witten conformal field theory [1], and this has an SO(4) = [SU(2) × SU(2)]/$\mathbb{Z}_2$ symmetry which is much larger than the global symmetry present microscopically.

Physically, this arises as follows [2]. The Néel vector $\vec{N}$ has three components. There is also a spin-Peierls order parameter φ which distinguishes between the two different patterns of dimer (singlet) order, and which changes sign under appropriate reflections or translations. We may form the 4-component superspin $\vec{\Phi} = (\vec{N}, \varphi)$, and the emergent SO(4) corresponds to rotations of this vector. Although the dimer and Néel order parameters are utterly inequivalent microscopically, a symmetry between them arises in the infra-red. Technically, this again relies on the SO(4)–breaking perturbations of the conformal field theory being irrelevant or marginally irrelevant.

Naively one might expect this phenomenon to be special to one spatial dimension, where the enlarged symmetry is related to special properties of 2D conformal invariance (the doubling of conserved currents [1]). We show here however that an analogous symmetry enhancement occurs for the spin-1/2 magnet on the square lattice, at the celebrated 'deconfined' quantum critical point [3–5]. This is a transition between the antiferromagnetically ordered Néel state and a columnar valence-bond-solid (VBS), and is reached by tuning a single parameter. For example, the nearest-neighbour Heisenberg model can be driven into the VBS using either a four-spin interaction [7] or a next–nearest–neighbour exchange [6, 8]. The emergent symmetry we put forward is an SO(5) which mixes the components of the Néel vector $\vec{N}$, which has three components, and the VBS order parameter $\vec{\varphi}$, which has two. We test it by examining the joint probability distribution for these quantities.

Numerically, the critical behaviour can be studied efficiently with a 3D classical loop model [9], and we use this approach here. The order of the transition has been controversial as a result of violations of conventional finite–size scaling [10–15] which we discussed in detail previously [9]. We will return to this below, arguing that the present results support the continuity of the transition.

The Néel–VBS transition is usually described with the non-compact CP^1 (NCCP^1) Lagrangian [4, 16],

$$\mathcal{L} = |(\nabla - iA)\boldsymbol{z}|^2 + \kappa(\nabla \times A)^2 + \mu|\boldsymbol{z}|^2 + \lambda|\boldsymbol{z}|^4. \quad (1)$$

The two-component bosonic spinon field $\boldsymbol{z} = (z_1, z_2)$ is related to the Néel vector $\vec{N}$ by $\vec{N} = \boldsymbol{z}^\dagger \vec{\sigma} \boldsymbol{z}$. The U(1) gauge field A_μ is related by duality to the VBS order parameter $\vec{\varphi} = (\varphi_x, \varphi_y)$ which distinguishes the different columnar singlet patterns [4, 17]. Although we will use the language of the Néel–VBS transition, our conclusions apply more generally to the above field theory, and indicate that it flows to an SO(5)–symmetric fixed point at the critical value of μ. In the language of this 3D gauge theory, the VBS order parameter is the operator $\mathcal{M} = \varphi_x + i\varphi_y$ which inserts a Dirac monopole in A_μ [4, 18, 19].

SO(5) symmetry cannot be made explicit in the formulation of Eq. 1. Fortunately, Senthil and Fisher [20],
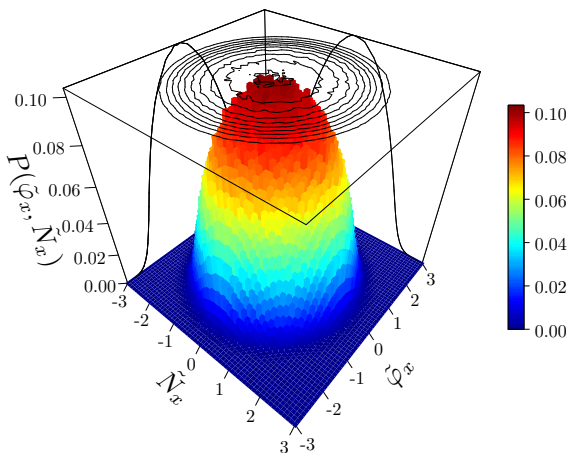
FIG. 1. The joint probability distribution $P(\widetilde{N}_x, \widetilde{\varphi}_x)$, after rescaling N_x and φ_x to have unit variance, in a critical system of size $L = 100$. Upper plane shows contour plot.

building on work of Tanaka and Hu [21], have argued that an alternative field theory describes the Néel–VBS transition and is equivalent to Eq. 1. This is a nonlinear σ-model (NLσM) for the five-component superspin

$$\vec{\Phi} = (N_x, N_y, N_z, \varphi_x, \varphi_y), \qquad (2)$$

augmented with: (i) anisotropies that break the global symmetry from SO(5) down to the spin rotation and spatial symmetries present microscopically; and (ii) a topological Wess–Zumino–Witten term at level one [22, 23], which is analogous to that in the CFT for the spin chain. The leading anisotropy plays the role of the mass term in Eq. 1: it drives the transition between the Néel and VBS ordered phases.

The NLσM formulation makes the emergent symmetry a more natural possibility, since it could arise at the critical point if all the higher anisotropies happen to be renormalisation–group irrelevant. We will discuss below the phase diagram for the NLσM (with WZW term) which is implied by this conjecture.

In previous work we characterised various observables at the deconfined transition in detail, using a three-dimensional loop representation to reach system sizes up to $L = 512$. See Ref. [9] for details of the model, which is in the Néel phase for coupling $J < J_c$ and the VBS phase for $J > J_c$, with $J_c = 0.088501(3)$. We found a remarkable similarity between the critical Néel and VBS correlation functions. The anomalous dimensions determined from the correlators at separations $r \ll L$ are $\eta_{\text{Néel}} = 0.259(6)$ and $\eta_{\text{VBS}} = 0.25(3)$ [24]; the two correlators also behave similarly in the regime $r \sim L$ (despite the scaling violations discussed in Ref. [9]). This suggests searching for an emergent SO(5) symmetry that would explain these apparent coincidences.

Probability distribution. Consider the joint distribution for the Néel and VBS order parameters in a system of linear size L. If SO(5) emerges, then this will be a

function only of $\vec{\Phi}^2 = \vec{N}^2 + \vec{\varphi}^2$ at the critical point (after a trivial rescaling of $\vec{\varphi}$). Spin rotation symmetry of course already guarantees that the distribution depends on $\vec{N}$ only via $\vec{N}^2$. Also, while microscopic spatial symmetry only allows $\vec{\varphi}$ to rotated by multiples of $\pi/2$, it is well established numerically that symmetry under continuous U(1) rotations of $\vec{\varphi}$ emerges close to the transition [25, 26]. This was checked for the present model in Ref. [9] (see also App. B, and see Ref. [27] for related phenomena). The crucial point is therefore whether the distribution is invariant under U(1) rotations that mix a component of $\vec{\varphi}$ with a component of $\vec{N}$.

Let the standard deviations of N_x and φ_x be denoted σ_N and σ_φ respectively, and use a tilde to denote quantities rescaled to have unit variance: $\widetilde{N}_x = N_x/\sigma_N$ and $\widetilde{\varphi}_x = \varphi_x/\sigma_\varphi$. Fig. 1 shows the joint probability distribution for these quantities at the critical point $J = J_c$ in a system of size $L = 100$. The visual evidence for emergent symmetry between Néel and VBS is striking.

Before turning to a quantitative analysis of the distribution, a basic test is that the variances σ_N and σ_φ of the order parameters depend on system size in the same way at criticality [28], i.e. that σ_φ/σ_N is L-independent at J_c. In Fig. 2 this is confirmed to high precision over a wide range of lengthscales. Plots of σ_φ/σ_N versus J for different L-values cross at J_c [29] (the value of σ_φ/σ_N at J_c depends on the nonuniversal normalisation of the lattice operators).

For a quantitative analysis of the probability distribution we examine the moments

$$F_\ell^a = \langle r^a \cos(\ell\theta) \rangle, \qquad (3)$$

where $(\widetilde{N}_x, \widetilde{\varphi}_x) = r(\cos\theta, \sin\theta)$. Emergent symmetry requires these to vanish for $\ell > 0$. We have computed F_2^4
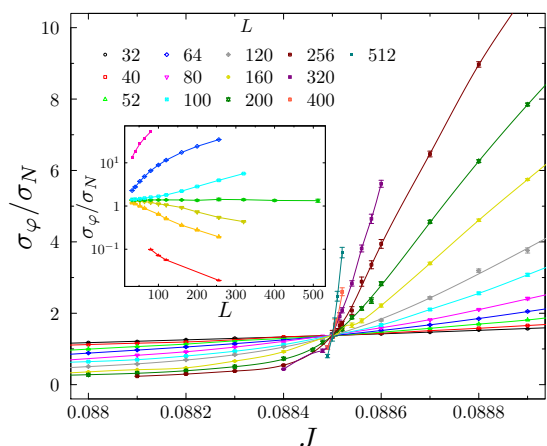

FIG. 2. Main panel: variance ratio σ_φ/σ_N plotted against J for various L. Curves cross at J_c as expected from SO(5) symmetry. Inset: same quantity as a function of L for several J around $J_c \simeq 0.0885$ (key in Fig. 3).

and F_4^4 for large sizes:

$$F_2^4 = \left\langle \widetilde{N}_x^4 - \widetilde{\varphi}_x^4 \right\rangle, \quad F_4^4 = \left\langle \widetilde{N}_x^4 - 6\widetilde{N}_x^2\widetilde{\varphi}_x^2 + \widetilde{\varphi}_x^4 \right\rangle. \quad (4)$$

Fig. 3 shows these as a function of L at and close to the critical point. Both are consistent with zero for $J = J_c$ over the whole range of L. The expected values in the adjacent phases (including the regime of weak VBS order, where there is an effective U(1) symmetry for rotations of $\vec{\varphi}$) are also indicated in the figure (details in App. B).

In Fig. 4 we show F_2^4 as a function of J: note the very clearly defined crossing at $J = J_c$, $F_2^4 = 0$. Further moments are shown for $L = 100$ in App. B. It should be noted that the critical distribution is markedly non-Gaussian, with nonvanishing higher cumulants such as $[\langle N_x^4 \rangle - 3\langle N_x^2 \rangle^2]/\langle N_x^2 \rangle^2 = -0.7549(13)$ (for $L = 100$).

Equalities between scaling dimensions. In addition to the equivalence between Néel and VBS vectors (manifested in the joint distribution and the anomalous dimensions), SO(5) has consequences for operators transforming in higher representations. Take the leading operators in the symmetric two– and four–index representations:

$$\mathcal{O}_{ab}^{(2)} = \Phi_a\Phi_b - \tfrac{1}{5}\delta_{ab}\Phi^2, \quad \mathcal{O}_{abcd}^{(4)} = \Phi_a\Phi_b\Phi_c\Phi_d - C_{abcd}.$$

The subtractions [30] ensure the operators transform irreducibly. $\mathcal{O}^{(2)}$ is relevant, with scaling dimension $x_2 < 3$. In fact a component of $\mathcal{O}^{(2)}$ is the operator $\mathcal{O}_J$ which drives us through the Néel–VBS transition as we vary J, by favouring one or the other order ($\mathcal{O}_J$ therefore plays the role of the mass term in Eq. 1):

$$\mathcal{O}_J = \tfrac{5}{2}\sum_{a=1}^{3}\mathcal{O}_{aa}^{(2)} = \vec{N}^2 - \tfrac{3}{2}\vec{\varphi}^2. \quad (5)$$

Remarkably, various *a priori* unrelated operators share the same scaling dimension x_2 since they are also com-
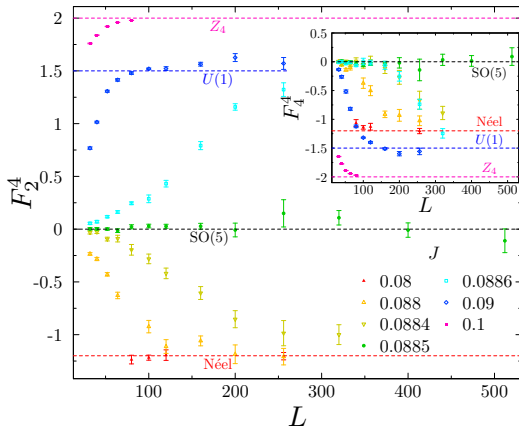
FIG. 3. Moments F_2^4 (main panel) and F_4^4 (inset) defined in Eq. 4, shown as a function of L for a few values of J at and close to $J_c \simeq 0.0885$. Dashed lines indicate expected values in the Néel phase, at the SO(5)–symmetric critical point, and in the U(1) and $\mathbb{Z}_4$–symmetric regimes of the VBS phase.
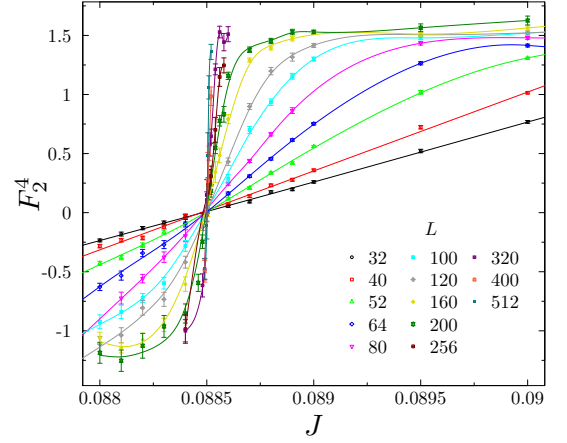
FIG. 4. F_2^4 (Eq. 4) as a function of J for various sizes, showing a crossing at $F_2^4 = 0$, $J = J_c$ as expected for SO(5) symmetry.

ponents of $\mathcal{O}^{(2)}$. These include the spin–quadrupole moments, $N_aN_b - \delta_{ab}\vec{N}^2/3$, and the relevant [26] operators $\varphi_a\varphi_b - \delta_{ab}\vec{\varphi}^2/2$ which in the NCCP^1 language insert 'strength-two' monopoles [40]. Even more oddly, the same scaling dimension controls φ_aN_b, despite the fact that microscopically this operator is as dissimilar from $\mathcal{O}_J$ as possible — φ_aN_b transforms under both spin and spatial symmetries, while $\mathcal{O}_J$ is invariant under them.

To test these predictions, Fig. 5 shows data for the two-point functions of $\mathcal{O}_J$, φ_xN_z, and $\varphi_x\varphi_y$, or rather lattice versions of these operators. (See App. A for definitions and Ref. [9] for a general discussion of correlation functions at the critical point.) Note the striking similarity of the three curves, as expected from SO(5). The slopes at $r \sim 10$ are around $x_2^{\mathrm{eff}} \sim 1.5$, but this effective exponent may be strongly affected by finite size effects. (Various scaling dimensions, including the two-monopole dimension [31], are known at large n in the SU(n) generalisation of Eq. 1 [32–35], and show that a symmetry between Néel and VBS cannot persist in this limit.)

$\mathcal{O}^{(4)}$ allows us to write both a subleading operator which breaks the symmetry between Néel and VBS ($\sum_{a=1}^{3}\sum_{b=4}^{5}\mathcal{O}_{aabb}^{(4)}$), and one which breaks the remaining symmetry for $\vec{\varphi}$ down to fourfold rotations ($\sum_{a=4}^{5}\mathcal{O}_{aaaa}^{(4)}$). Therefore it is possible that the same irrelevant exponent controls finite-size corrections to both types of symmetry enhancement (see also App. B).

Nonlinear σ–model. The NLσM description of the deconfined critical point proposed in Ref. [20] is

$$S_\sigma = \int \mathrm{d}^3x\left(\frac{1}{g}\big(\nabla\vec{\Phi}\big)^2 + \sum_i \lambda_i\mathcal{O}_i\right) + S_{\mathrm{WZW}} \quad (6)$$

where S_{WZW} is a topological Wess-Zumino-Witten term at level one (associated with the homotopy group $\pi_4(S^4) = \mathbb{Z}$ of the target space). Physically, this term ensures that a vortex in the VBS order has an unpaired spin–1/2 at its core [17, 20]. The $\mathcal{O}_i$ are the various

anisotropies, some discussed above, that break SO(5) symmetry down to the microscopic physical symmetry.

Suppose that the Néel–VBS transition is continuous, with emergent SO(5) symmetry, and that the NLσM is a viable description of this transition. Since the critical point is reached by tuning a single parameter, there is only a *single* RG–relevant coupling in Eq. 6, namely the anistotropy $\mathcal{O}_J$ of Eq. 5. Therefore the SO(5)—symmetric NLσM, with no anisotropies, has a nontrivial infra-red *stable* fixed point controlling a power-law correlated phase: see Fig. 6. This fixed point then also governs the deconfined transition. (The NLσM also has a stable ordered phase even in the presence of the WZW term.)

The phase diagram of Fig. 6 is counterintuitive, as we are used to 3D σ–models with an ordered phase, a trivial disordered phase, and an unstable critical point in between. But that conventional picture applies to the NLσM without a WZW term. The present results indicate that the WZW term causes the trivial disordered phase to be replaced with a stable critical phase. While the absence of a trivial disordered phase may seem surprising, it is in fact a necessary feature of any field theory which faithfully describes the spin-1/2 magnet, as argued in Ref. [20]. By the 2D generalisation of the Lieb-Schultz-Mattis theorem [36, 37], the magnet cannot be in a trivially disordered phase with a unique, symmetric, gapped ground state (it can be critical, or topologically ordered, or spontaneously break a symmetry). Thus the field theory should not have such a trivial phase either [41]. This argument does not by itself imply the existence of a stable critical phase, only the absence of a trivial fully disordered one. (See Refs. [20, 38] for related discussions of the SO(4) case.)

The emergent SO(5) therefore indicates the existence of a 3D SO(5)–symmetric CFT which is radically unlike standard Wilson-Fisher CFTs, in that there are no relevant singlet operators. It would be very interesting to investigate this using the conformal bootstrap [42], making use of numerical estimates for operator dimensions
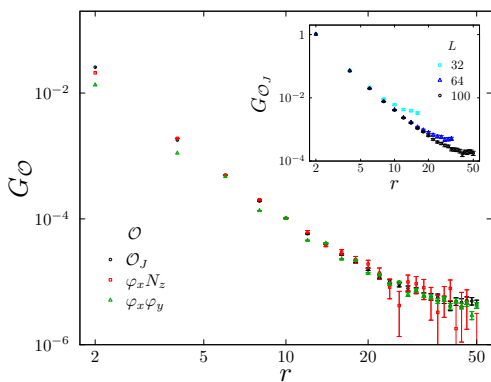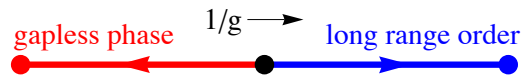

FIG. 6. Conjectured phase diagram for NLσM with WZW term in presence of full SO(5) symmetry. The fixed point on the left also governs the deconfined critical point, where SO(5) is emergent. Moving away from J_c introduces the relevant symmetry-breaking perturbation $\mathcal{O}_J$, leading to the Néel or VBS phase.

[9]. This should be simpler [43] than studying the critical NCCP^1 model without assuming SO(5).

Scaling violations. The deconfined critical point shows strong violations of finite-size scaling. We argued in Ref. [9] that these are *not* simply large corrections to scaling of the conventional type (i.e. from irrelevant or marginally irrelevant operators), but should instead be attributed *either* to a first order transition with an anomalously large correlation length *or* to a genuine critical point with unconventional finite-size scaling due to a dangerously irrelevant variable. The present results strongly suggest the second scenario — a genuine continuous transition. This is because a critical point is the only natural explanation for the emergent SO(5) symmetry, which we have tested here to high precision. This symmetry therefore provides long-sought direct evidence that the deconfined transition is continuous.

In more detail: if one attempts to account for the data in terms of an anomalously weak first order transition (i.e. without postulating a genuine 3D critical point), one is led to a scenario where the apparent critical behaviour is due to a 'nearby' fixed point at spacetime dimension slightly *below* three [9]. While this scenario can potentially explain pseudo-critical behaviour up to an extremely large lengthscale, it cannot account for the emergent SO(5) symmetry — this makes sense only for a 3D fixed point. While we can consider the NCCP^1 model in arbitrary dimension, the operator $\vec{\varphi}$ (interpreted for example as a monopole insertion operator) is special to 3D, and is required for construction of the SO(5) superspin.

Assuming therefore that the transition is continuous, a possible explanation for the scaling violations is that a dangerously-irrelevant variable is required to cut off the fluctuations of a zero mode of the field [9]. (This would be analogous to ϕ^4 theory above four dimensions, where the quartic term is irrelevant, but cannot be set to zero since it is needed to prevent divergent fluctuations of ϕ's zero mode [44].) This may suggest that an alternative field theory description exists which is more natural than the NLσM [39].

Future directions. It would be interesting to investigate consequences of the emergent symmetry for finite temperature behaviour, as well as to look for signs of it using methods complimentary to Monte Carlo such as exact diagonalisation or DMRG. The present results also motivate further analysis of SO(5)–symmetric 3D CFTs — for example with the conformal bootstrap — and a

FIG. 5. Correlators $G_{\mathcal{O}}(r)$ for operators $\varphi_x N_z$, $\varphi_x \varphi_y$ and $\mathcal{O}_J$ in a system of size $L = 100$. (The $G_{\mathcal{O}}$ have been normalised to agree at $r = 10$.) Inset: $G_{\mathcal{O}_J}$ for various L.

more general investigation of the role played by WZW terms in field theories above two dimensions. For example, is there an analogous SO(6)–symmetric CFT in 4D? Finally, we note that the critical behaviour at the deconfined transition remains perplexing, and deserves further investigation.

Appendix A: Lattice definitions of operators

We refer to the lattice field theory of Ref. [9], described there for $J = 0$ but modifiable for $J \neq 0$. The Néel vector N is defined on each link by $\vec{N} = \boldsymbol{z}^\dagger \vec{\sigma} \boldsymbol{z}$ with $|\boldsymbol{z}|^2 = 2$ (these normalisations are purely a matter of convenience). A graphical expansion maps the lattice field theory to a partition function for loops taking two colours, red and blue [45]. Inserting operators on the links modifies the graphical expansion. Using $\operatorname{Tr} N_z z_c z_d^* = (2/3)\delta_{cd}(\delta_{c1} - \delta_{c2})$, where Tr is the integral over $\boldsymbol{z}$s and $\operatorname{Tr} z_c z_d^* = \delta_{cd}$, one may check that N_z is simply the operator which measures the colour of a link in the loop gas: $N_z = (2/3)\chi$, where χ is ± 1 depending on whether the link is red or blue. Therefore we obtain the probability distribution for the z-component of the uniform magnetisation, N_z^{tot} by measuring the number of red links in the Monte Carlo simulation. We may measure $\vec{\varphi}$ simultaneously, allowing construction of the joint probability distribution. This is what we have done for system sizes $L \leq 100$. (In the main text the component we singled out was labelled N_x rather than N_z, but of course by symmetry there is no difference.)

For larger system sizes we do not have data for the full probability distribution of link colours. However we have data for low moments of the loop length distribution, and this is sufficient to construct the moments F_2^4 and F_4^4 shown above. We define, in a given configuration,

$$S_k = \sum_{\text{loops}} (\text{length of loop})^k. \tag{A1}$$

The necessary relations follow straightforwardly from $\sum_{\text{links}} N_z = (2/3) \sum_{\text{links}} \chi$. We express $\langle (N_z^{\text{tot}})^s \rangle$ as a correlation function of χ operators in the loop gas. Summing over the possible colourings of a given loop configuration gives a nonzero result only if there are an even number of χ insertions on each loop. Taking into account the possible ways of assigning χs to loops, we have

$$\langle (N_z^{\text{tot}})^2 \rangle = (2/3)^2 \langle S_2 \rangle, \tag{A2}$$

$$\langle (N_z^{\text{tot}})^4 \rangle = (2/3)^4 \langle 3S_2^2 - 2S_4 \rangle. \tag{A3}$$

F_l^a	$a = 0$	$a = 2$	$a = 4$	$a = 6$
$l = 2$	0.00035(17)	0.000(4)	0.00(2)	0.01(7)
$l = 4$	0.0002(7)	-0.001(2)	-0.004(8)	-0.02(3)
$l = 6$	0.0002(5)	0.000(1)	-0.003(5)	-0.02(2)

TABLE I. Moments F_l^a in the $(\widetilde{N}_x, \widetilde{\varphi}_x)$ plane for $L = 100$ (taken at $J = 0.0885$).
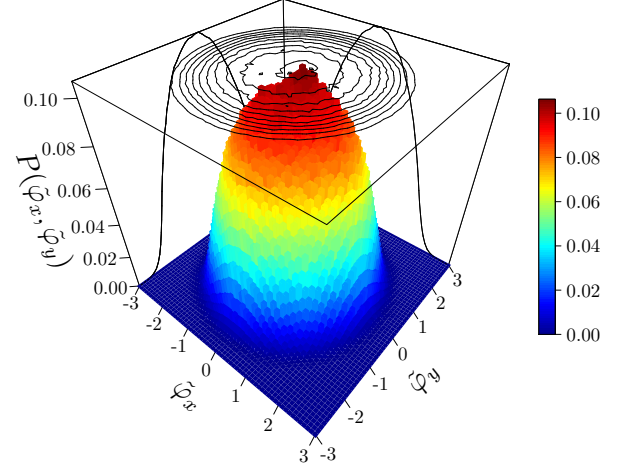

FIG. 7. The joint probability distribution $P(\widetilde{\varphi}_x, \widetilde{\varphi}_x)$, after rescaling φ_x and φ_y to have unit variance, in a critical system of size $L = 100$. Upper plane shows contour plot.

Importantly, these relations remain true if powers of $\vec{\varphi}$ are inserted on the left and right hand sides. This allows us to construct the abovementioned moments.

Note that in order to give optimal statistics, the uniform magnetisation/VBS order is always defined by an integral over the three-dimensional sample — i.e. space-time, in the quantum language — rather than a two-dimensional 'spatial' slice.

The 3D 'L' lattice [46] on which the model is defined is bipartite, with φ_x defined at nodes of the A sublattice and φ_y at nodes of the B sublattice, and the Boltzmann weight couples nearest neighbour φ components on the same sublattice [9]. The operators whose correlation functions are plotted in Fig. 5 are all defined at a node, and the correlation functions are evaluated for pairs of nodes on the same sublattice, separated parallel to a coordinate direction. We define $\mathcal{O}_J(r)$ as the sum of the eight terms in the lattice energy which involve the node r, and subtract the average so that $\langle \mathcal{O}_J \rangle = 0$. The operator $[\varphi_x \varphi_y](r)$ is defined as the sum of $\varphi_x(r)\varphi(r')$ over the four nearest neighbours r' of r (see Fig. 1 in Ref. [9]) and $[\varphi_x N_z](r)$ is defined as the sum of $\varphi_x(r)N_z(l)$ over the four links l connected to r, with N_z defined as above in terms of link colours. Each of these operators is therefore supported on star: we take the separation of the two points in the correlator to be perpendicular to the plane of the stars.

Appendix B: Additional data for probability distribution

Table I shows data for a variety of the moments F_l^a defined in Eq. 3 in a system of size $L = 100$ at $J = 0.0885$. These quantify the U(1) symmetry of the distribution in the $(\widetilde{N}_x, \widetilde{\varphi}_x)$ plane. All are consistent with zero.

L	$a = 0$	$a = 2$	$a = 4$	$a = 6$
32	-0.0086(9)	-0.035(3)	-0.166(10)	-0.88(5)
64	-0.005(1)	-0.021(3)	-0.095(11)	-0.48(5)
100	-0.0028(14)	-0.014(4)	-0.069(15)	-0.35(7)

TABLE II. Moments $\widetilde{F}_4^a$ in the $(\widetilde{\varphi}_x, \widetilde{\varphi}_y)$ plane, quantifying fourfold anisotropy for the VBS, for $L = 32, 64, 100$. (Note that moments grow with a for trivial reasons.)

We also examine the symmetry properties of the probability distribution in the $(\widetilde{\varphi}_x, \widetilde{\varphi}_y)$ plane. This is shown in Fig. 7 for a critical system of size 100. Again it is U(1) symmetric to an excellent approximation. Interestingly though, the finite-size corrections to this U(1) are larger than those for the U(1) in the $(\widetilde{N}_x, \widetilde{\varphi}_x)$ plane (but still small). Table II quantifies fourfold anisotropy for the VBS at the critical point via the moments $\widetilde{F}_4^a$ (defined analogously to F_l^a but in the $(\widetilde{\varphi}_x, \widetilde{\varphi}_y)$ plane). They decrease with system size roughly as L^{-c} with $c \sim 0.8$.

In Fig. 3 of the main text the straight lines indicate the expected values of the moments F_2^4 and F_4^4 within the phases. These values follow straightforwardly. The vector which is in disordered phase has a Gaussian distribution, so its moments follow from Wick's theorem. The other order parameter can be treated as fixed in magnitude and averaged over symmetry-equivalent directions. In the Néel phase this gives $F_2^4 = F_4^4 = -1.2$. Our choice of coordinates is such that deep in the VBS phase $\vec{\varphi} \propto (\pm 1, \pm 1)$, which gives $F_2^4 = 2$, $F_4^4 = -2$. For weak VBS order there is a large range of L where U(1) symmetry for $\vec{\varphi}$ survives, and $F_2^4 = 1.5$, $F_4^4 = -1.5$.

[1] I. Affleck, *Critical Behaviour of Two-Dimensional Systems with Continuous Symmetries,* Phys. Rev. Lett. **55**, 1355 (1985).

[2] A. M. Tsvelik, *Quantum Field theory in Condensed Matter Physics*, Cambridge University Press, 2nd ed. 2003.

[3] T. Senthil, A. Vishwanath, L. Balents, S. Sachdev, and M. P. A. Fisher, *Deconfined Quantum Critical Points*, Science **303**, 1490 (2004).

[4] T. Senthil, L. Balents, S. Sachdev, A. Vishwanath, and M. P. A. Fisher, *Quantum criticality beyond the Landau-Ginzburg-Wilson paradigm*, Phys. Rev. B **70**, 144407 (2004).

[5] T. Senthil, L. Balents, S. Sachdev, A. Vishwanath, and M. P. A. Fisher, *Deconfined Criticality Critically Defined*, J. Phys. Soc. Jpn. **74** Suppl. 1 (2005).

[6] L. Wang, Z.-C. Gu, F. Verstraete, and X.-G. Wen, *Spin-liquid phase in spin-1/2 square $J_1 - J_2$ Heisenberg model: A tensor product state approach,* arXiv:1112.3331, v3 (2015).

[7] A. W. Sandvik, *Evidence for Deconfined Quantum Criticality in a Two-Dimensional Heisenberg Model with Four-Spin Interactions*, Phys. Rev. Lett. **98**, 227202 (2007).

[8] A. W. Sandvik, *Finite-size scaling and boundary effects in two-dimensional valence-bond solids,* Phys. Rev. B **85**, 134407 (2012).

[9] A. Nahum, J. T. Chalker, P. Serna, M. Ortuño and A. M. Somoza, *Deconfined Quantum Criticality, Scaling Violations, and Classical Loop Models*, arXiv:1506.06798 (2015).

[10] A. W. Sandvik, *Continuous Quantum Phase Transition between an Antiferromagnet and a Valence-Bond Solid in Two Dimensions: Evidence for Logarithmic Corrections to Scaling*, Phys. Rev. Lett. **104**, 177201 (2010).

[11] F. J. Jiang, M. Nyfeler, S. Chandrasekharan, and U. J. Wiese, *From an antiferromagnet to a valence bond solid: evidence for a first-order phase transition*, J. Stat. Mech. P02009 (2008).

[12] A. Banerjee, K. Damle, and F. Alet, *Impurity spin texture at a deconfined quantum critical point*, Phys. Rev. B **82**, 155139 (2010).

[13] K. Chen. Y. Huang, Y. Deng, A. B. Kuklov, N. V. Prokof'ev, and B. V. Svistunov, *Deconfined Criticality Flow in the Heisenberg Model with Ring-Exchange Interactions*, PRL **110**, 185701 (2013).

[14] K. Harada, T. Suzuki, T. Okubo, H. Matsuo, J. Lou, H. Watanabe, S. Todo, and N. Kawashima, *Possibility of deconfined criticality in $SU(N)$ Heisenberg models at small N*, Phys. Rev. B. **88**, 220408 (2013).

[15] R. K. Kaul, *Quantum criticality in $SU(3)$ and $SU(4)$ antiferromagnets*, Phys. Rev. B **84** 054407 (2011).

[16] O. I. Motrunich and A. Vishwanath, *Emergent photons and transitions in the $O(3)$ sigma model with hedgehog suppression*, Phys. Rev. B **70**, 075104 (2004).

[17] M. Levin and T. Senthil, *Deconfined quantum criticality and Néel order via dimer disorder*, Phys. Rev. B **70**, 220403 (2004).

[18] F. D. M. Haldane, *$O(3)$ Nonlinear σ Model and the Topological Distinction between Integer- and Half-Integer-Spin Antiferromagnets in Two Dimensions,* Phys. Rev. Lett. **61**, 1029 (1988).

[19] N. Read and S. Sachdev, *Valence-bond and spin-Peierls ground states of low dimensional quantum antiferromagnets,* Phys. Rev. Lett. **62**, 1694 (1989).

[20] T. Senthil and M. P. A. Fisher, *Competing orders, nonlinear sigma models, and topological terms in quantum magnets*, Phys. Rev. B **74**, 064405 (2006).

[21] A. Tanaka and X. Hu, *Many-Body Spin Berry Phases Emerging from the π-Flux State: Competition between Antiferromagnetism and the Valence-Bond-Solid State,* Phys. Rev. Lett. **95**, 036402 (2005).

[22] G. Ferretti and S. G. Rajeev, *Current algebra in three dimensions*, Phys. Rev. Lett. **69**, 2033 (1992).

[23] A. G. Abanov and P. B. Wiegmann, *Theta-terms in non-linear sigma-models,* Nucl. Phys. B **570**, 685 (2000).

[24] Early numerical work suggested that $\eta_{\text{Néel}} = \eta_{\text{VBS}}$ [7], but this was subsequently questioned [25].

[25] J. Lou, A. Sandvik and N. Kawashima, *Antiferromagnetic to valence-bond-solid transitions in two-dimensional $SU(N)$ Heisenberg models with multispin interactions*, Phys. Rev. B **80**, 180414 (2009).

[26] M. S. Block, R. G. Melko, and R. K. Kaul, *Fate of CP^{n-1} Fixed Points with q Monopoles*, Phys. Rev. Lett. **111**, 137202 (2013).

[27] G. Misguich, V. Pasquier, and F. Alet, *Correlations and order parameter at a Coulomb-crystal phase transition in a three-dimensional dimer model*, Phys. Rev. B **78**, 100402(R) (2008).

[28] At a conventional critical point, L-independence of σ_φ/σ_N would be equivalent to equality of η_{VBS} and $\eta_{\text{Néel}}$, but finite-size scaling may be unconventional here [9].

[29] Attempting to collapse this data using a correlation length exponent ν gives a drift in ν comparable to those in Sec. IV E of Ref. [9].

[30] $C_{abcd} = \left[7\Phi^2 \left(\Phi_a\Phi_b\delta_{cd} + \ldots \right) - (\Phi^2)^2 \left(\delta_{ab}\delta_{cd} + \ldots \right) \right] /63$.

[31] E. Dyer, M. Mezei, S. S. Pufu, and S. Sachdev, *Scaling Dimensions of Monopole Operators in the CP^{n-1} Theory in $2+1$ dimensions*, arXiv:1504.00368 (2015).

[32] G. Murthy and S. Sachdev, *Action of hedgehog instantons in the disordered phase of the $(2+1)$-dimensional CP^{N-1} model*, Nucl. Phys. B **344**, 557 (1990).

[33] R. K. Kaul and S. Sachdev, *Quantum criticality of $U(1)$ gauge theories with fermionic and bosonic matter in two spatial dimensions*, Phys. Rev. B 77, 155105 (2008).

[34] M. A. Metlitski, M. Hermele, T. Senthil and M. P. A. Fisher, *Monopoles in CP^{N-1} model via the state-operator correspondence*, Phys. Rev. B **78**, 214418 (2008).

[35] R. Kaul and A. Sandvik, *Lattice Model for the $SU(N)$ Néel to Valence-Bond Solid Quantum Phase Transition at Large N*, Phys. Rev. Lett. **108**, 137201 (2012).

[36] M. B. Hastings, *Lieb-Schultz-Mattis in higher dimensions*, Phys. Rev. B **69**, 104431 (2004).

[37] E. H. Lieb, T. D. Schultz, and D. C. Mattis, *Two soluble models of an antiferromagnetic chain*, Ann. Phys. (N. Y.) **16**, 407 (1961).

[38] C. Xu and A. W. W. Ludwig, *Nonperturbative Effects of a Topological Theta Term on Principal Chiral Nonlinear Sigma Models in 2+1 Dimensions*, Phys. Rev. Lett. **110**, 200405 (2013).

[39] A. Nahum and T. Senthil, in preparation.

[40] This operator (specifically $\varphi_x^2 - \varphi_y^2$) also implements rectangular anisotropy in the Heisenberg magnet.

[41] The anisotropies are not important for this argument since if a trivial disordered phase existed in their absence it should be stable to their inclusion [20].

[42] F. Kos, D. Poland, and D. Simmons-Duffin, *Bootstrapping the $O(N)$ vector models*, JHEP **1406** 091, (2014).

[43] If only SO(3) symmetry is assumed the theory must be treated as a high-order multicritical point, as in addition to the relevant mass term there are relevant SO(3)-invariant operators for single/double monopoles. (Lattice symmetry forbids them at the Néel-VBS transition.)

[44] E. Brézin and J. Zinn-Justin, *Finite Size Effects in Phase Transitions*, Nucl. Phys. B **257**, 867 (1985).

[45] A. Nahum, J. T. Chalker, P. Serna, M. Ortuño and A. M. Somoza, *Phase transitions in 3D loop models and the CP^{n-1} sigma model*, Phys. Rev. B **88**, 134411 (2013).

[46] J. Cardy, *Quantum Network Models and Classical Localization Problems*, in *50 Years of Anderson Localization*, E. Abrahams, ed. (World Scientific, Singapore, 2010).